Available online at www.sciencedirect.com
SCIENCE DIRECT®
Radiation Physics and Chemistry 71 (2004) 683–692
Radiation Physics and Chemistry
www.elsevier.com/locate/radphyschem

Detectors for medical radioisotope imaging: demands and perspectives

M.I. Lopes[a,b,*], V. Chepel[a,b]

[a] LIP—Laboratório de Instrumentação e Física Experimental de Partículas, Universidade de Coimbra, Coimbra, Portugal
[b] C.F.R.M. do Departamento de Física, Universidade de Coimbra, 3004-516 Coimbra, Portugal

Abstract

Radioisotope imaging is used to obtain information on biochemical processes in living organisms, being a tool of increasing importance for medical diagnosis. The improvement and expansion of these techniques depend on the progress attained in several areas, such as radionuclide production, radiopharmaceuticals, radiation detectors and image reconstruction algorithms. This review paper will be concerned only with the detector technology.

We will review in general terms the present status of medical radioisotope imaging instrumentation with the emphasis put on the developments of high-resolution gamma cameras and PET detector systems for scinti-mammography and animal imaging. The present trend to combine two or more modalities in a single machine in order to obtain complementary information will also be considered.

Keywords: Medical imaging; Gamma camera; PET; SPECT; Radiation detectors

1. Introduction

Radioisotope medical imaging is a powerful diagnostic tool. The patient is injected with, or inhales, a small amount of a radioactive imaging agent, also referred to as a radiopharmaceutical, chosen to accumulate in the specific regions of the body under study. The imaging system then produces images of the resulting radiation patterns coming out of the body. One aims that these images reproduce, as accurately as possible, the distribution of radioactive agent uptake in the patient. Hence, nuclear medicine imaging provides information about organ functioning and physiology.

We can distinguish two types of radioisotope medical imaging techniques. Scintigraphy, i.e., planar imaging, and single photon emission computed tomography (SPECT), which provides a 3D image, both use radioisotopes that emit uncorrelated γ-photons of energy typically between 80 and 350 keV, ^{99m}Tc (140 keV γ-rays) being the most frequently employed. A detailed discussion of the radioisotope and radiopharmaceutical issues can be found, for instance, in Lima (1998). The other technique, positron emission tomography (PET), makes use of pairs of collinear photons emitted in the annihilation of a positron with an electron of the tissue, and, therefore is based on positron emitter radioisotopes. In the scintigraphy technique, a 2D projection of the emitting object to the detector is obtained by placing a position-sensitive detector of γ-rays and a collimator in front of it (with parallel holes, for example). In the tomographic techniques, it is possible to reconstruct a 3D image, which shows the distribution of the γ-emitter isotope throughout the organ(s) under study, by acquiring several 2D projections from different detector positions (Webb, 1998).

The detectors for radioisotope medical imaging operate in event counting mode. They have to detect gamma-rays of energy between 80 and 511 keV, depending on the technique, one by one, with the highest

*Corresponding author. C.F.R.M. do Departamento de Física, Universidade de Coimbra, 3004-516 Coimbra, Portugal. Tel.: +351-239410657; fax: +351-238822358.
E-mail address: isabel@lipc.fis.uc.pt (M.I. Lopes).

0969-806X/$ - see front matter © 2004 Elsevier Ltd. All rights reserved.
doi:10.1016/j.radphyschem.2004.04.058

possible efficiency and with a spatial resolution of the order of a few millimetres or even less. In addition, other requirements may be imposed, depending on the imaging technique and medical application.

The detector technology for radioisotope imaging has been dominated so far by two scintillating materials: NaI(Tl) for gamma cameras for scintigraphy and SPECT, and BGO (bismuth germanate $Bi_4Ge_3O_{12}$) for PET. In recent years, very remarkable advances in detection technology, namely concerning the development of new crystals, photodetectors and semiconductors, have been exploited for medical imaging. Some developments have already resulted in new devices that are already being commercialized. However, many of the ideas that have emerged are still in the proof-of-principle stage, aiming at arriving to the level of becoming ready for marketing.

This review paper is dedicated to the most recent detector technology associated with radioisotope medical imaging, in particular to some of the latest developments that have resulted from the advances in crystal production, new photodetectors and the progress achieved in the manufacture of semiconductors. As the area is very broad and many new proposals spring up every year, we had to restrict ourselves to some representative examples and no claim of completeness is made.

2. Gamma camera

Nearly all gamma cameras presently used for single-photon radioisotope imaging in nuclear medicine are based on the detector system proposed by Anger (1958), the so-called Anger camera, which consists of a large single NaI(Tl) crystal, typically 50 cm in diameter, optically coupled to an array of photomultiplier tubes. The interaction of a gamma-ray with the crystal results in a burst of isotropically emitted scintillation photons partially detected by the photomultipliers. Two coordinates of the position of the interaction are obtained from the amplitude distribution of the PMT signals and the energy is obtained from their sum. Both the position and energy resolutions are strongly determined by the number of detected scintillation photons per interacting gamma-ray. The intrinsic efficiency of detection is set by the thickness of the crystal. As the attenuation length of 140 keV photons in NaI is 4 mm, a crystal 12 mm thick assures more than 95% of interaction efficiency. Typical conventional Anger cameras have intrinsic spatial resolution of $\sim$3–5 mm (FWHM) and energy resolution of $\sim$9–11% (FWHM) for 140 keV gamma-rays, count rate capability up to $\sim 10^5$ cps.

Despite being a highly efficient and widely used instrument, the Anger camera, or improved variants present some limitations. In particular, they exhibit degradation of the position resolution towards the edge of the camera, non-uniformity and various forms of image distortion. Improvement in energy resolution would be desirable for a better discrimination of the gamma-rays that reach the detector after being scattered in the body because those events do not contain the correct position information and thus degrade the image contrast. Due to the bulky and heavy design of the conventional Anger camera, it is often difficult to position it as close to the organ as desired and to obtain the most suitable view. This difficulty is enhanced by the existence of a dead zone of several cm at the edges of the camera. The limitation in positioning the device is particularly important when imaging small organs as, for instance, in scinti-mammography, endocrinology and small animal imaging. For these applications, where the camera comes very close to the small object to be imaged, good position resolution is of prime importance.

The developments of new gamma cameras for scintigraphy and SPECT have been carried out along two main directions:

(1) The improvement of performance of the conventional large area (typically $40 \times 50\,cm^2$) gamma cameras, by optimizing the light collection and using recently developed position-sensitive photomultipliers or by using a completely different detection technique such as liquid and gas xenon detectors (Egorov et al., 1983; Nguen Ngoc et al., 1980; Bolozdynya et al., 1997).

(2) The development of compact, small area, task-specific gamma cameras.

Recently, the latter has received by far more interest in view of the importance of the applications involved. In fact, there has been an increasing interest in compact gamma cameras with high resolution over a small area. The main applications are scinti-mammography, animal imaging and intra-operative radio-guided surgery (RGS).

In view of these demands, new gamma cameras have been designed and tested. Among the technical solutions adopted, three have been intensively investigated: (a) a bundle of optically isolated crystal pillars read by a single position-sensitive photomultiplier (PSPMT); (b) modules composed by very thin crystals individually read out by PIN silicon photodiodes; (c) direct conversion of the gamma-rays into an electrical signal in pixelated semiconductor detectors with charge readout.

As for the scintillation crystals, CsI(Tl) and YAP:Ce (cerium-doped yttrium aluminium perovskite) have been investigated intensively due to their appropriate set of scintillation and gamma-rays attenuation properties (see Table 1) as well as their suitable physical and mechanical characteristics such as the absence of cleavage planes and low water absorption. Furthermore, they can be produced in the shape of long and thin pillars that can

Table 1
Some characteristics of the most used crystals in radioisotope medical imaging detectors (Knoll, 2000; Van Eijk, 2001)

	NaI(Tl)	CsI(Tl)	BaF_2	BGO	LSO:Ce	GSO:Ce	YAP:Ce	LuAP:Ce
Emission peak (nm)	410	565/420	310/220	480	420	440	360	365
Light yield (ph/keV)	38	65	11/1.5	8.2	25	9	18	12
Decay time								
Slow (ns)	230	680/3000	600	300		400		
Fast (ns)			0.8		40	60	27	17
Density (g/cm^3)	3.7	4.5	4.9	7.1	7.4	6.7	5.4	8.4
Chemical composition				$Bi_4Ge_3O_{12}$	Lu_2SiO_5	Gd_2SiO_5	$YAlO_3$	$LuAlO_3$
$1/\mu$ (cm) at 140 keV	0.41	0.28	0.29	0.086	0.11	0.16	0.7	0.1
$1/\mu$ (cm) at 511 keV	3.1	2.4	2.3	1.1	1.2	1.5	2.2	1.1
μ_{ph}/μ (%) at 511 keV	18	22	19	44	34	26	4.4	32

The total attenuation and absorption coefficients, μ and μ_{ph}, respectively, were calculated with XCOM (Berger et al., 1999) without including the coherent scattering. The detector materials are: NaI(Tl) and CsI(Tl)—thallium-doped sodium/caesium iodide, respectively; BGO—bismuth germinate; LSO:Ce and GSO:Ce—cerium-doped lutetium/gadolinium oxyorthosilicate, respectively; YAP:Ce and LuAP:Ce—yttrium/lutetium aluminium perovskite, respectively.

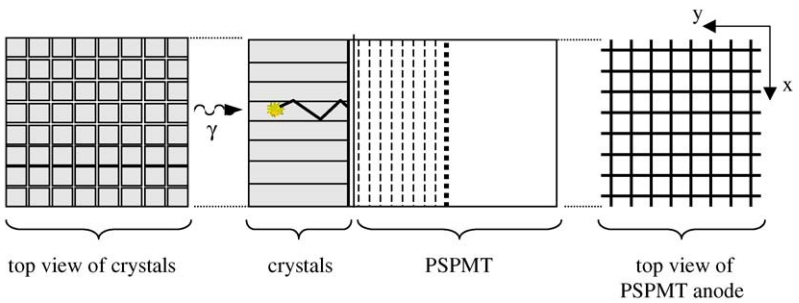

Fig. 1. Array of optically isolated crystals coupled to a position-sensitive photomultiplier (PSPMT) whose anode is composed of two planes of wires.

be arranged in compact multi-element configuration. NaI(Tl) is not suitable due to its hygroscopicity.

Fig. 1 shows schematically a gamma camera, which uses a multi-crystal matrix coupled to a PSPMT (Notaristefani et al., 1996; Pani et al., 1998). The gamma-ray interacts in one of the crystals and the scintillation photons produced there propagate along the pillar due to multiple reflections on the reflective layer that wraps each crystal. Hence, the pillar structure has the effect of focusing the scintillation light to a small spot on the photomultiplier photocathode. Owing to a special dynode structure, which preserves the spatial information on the photocathode illumination, the spread of the charge collected at the anode is very small. With a proper segmentation of the PMT anode, a good localization of the collected charge can be achieved. Therefore, a much better position resolution is expected from this system than that of a detector based on a single large crystal. Moreover, segmentation of the crystal leads to significantly fewer edge-effects than with a continuous crystal, provided that the photodetector has a uniform response over its active area. In Table 2, we list the characteristics of the crystal arrays and some of the performance parameters of two gamma cameras built using the concept discussed above. One of cameras was optimized for scinti-mammography and the other for small animal imaging.

Semiconductor detectors have long been viewed as a promising alternative to scintillators for gamma cameras as they have better energy resolution, can be easily pixelated and read out directly. Presently, the most attractive semiconductor material is cadmium zinc telluride, (CdZnTe or CZT as frequently abbreviated in the literature) as can be concluded from Table 3.

Table 2
Some characteristics of two compact gamma cameras, one designed for small animal imaging (YAPCAM) and the other for scinti-mammography (SPEM)

	YAPCAM[a]	SPEM[b]
Crystal type	YAP:Ce	CsI(Tl)
Total area (mm^2)	40×40	100×100
Single-crystal section (mm^2)	0.6×0.6	2×2
Crystal length (mm)	10	3
Crystal surface treatment	Reflective multi-layer	Epoxy diffuse layer
Inter-crystal space (mm)	0.01	0.3
PSPMT	Hamamatsu R2486	Hamamatsu R2392
PSPMT diameter (mm)	76	127
Intrinsic spatial resolution (mm)	0.5–0.9	1.8
Spatial resolution with collimator (mm)	1.5[c]	2[d]
Energy resolution (FWHM) (%)	40	23

The position and energy resolutions quoted are for 140 keV and 122 keV, respectively.
[a] Results summarized from Notaristefani et al. (1996).
[b] Results summarized from Maini et al. (1999).
[c] Collimators with circular holes of 0.9 mm diameter, septa of 0.25 mm and thickness of 30 and 20 mm were used.
[d] Collimator 35 mm thick with 1.7 mm hole diameter and a 0.2 mm septa thickness.

Table 3
Properties of some semiconductors at room temperature

	CdZnTe[a]	GaAs	Si
Effective atomic number	~ 50	32	14
Density (g/cm^3)	5.8	5.32	2.33
$1/\mu$ (for 140 keV γ-rays) (mm)	3	7.4	30
Electron mobility ($cm^2/V/s$)	1350	8500	1500
Hole mobility ($cm^2/V/s$)	120	400	450
Energy per electron–hole pair (eV)	4.7	4.2	3.61
Band gap (eV)	1.57	1.42	1.12
Resistivity (Ω cm)	$\sim 10^{11}$	$\sim 10^8$	$\sim 10^5$

[a] The properties of CdZnTe depend to some extent on the relative proportion of Zn and Cd.

Moreover, in recent years, a significant progress has been achieved in the growth of high-quality crystals, overcoming initial difficulties in achieving the required uniformity and absence of defects in the crystals (Squillante et al., 2001).

CdZnTe has very good absorption characteristics due to its high density and effective atomic number, the attenuation length of 140 keV gamma-rays being only 3 mm and the photofraction (μ_{ph}/μ) equal to 81%. It has a good charge yield (the full absorption of a 140 keV produces approximately 3×10^4 electrons) on the basis of which an excellent intrinsic energy resolution is expected. The high resistivity, due to the wide band gap, results in low leakage current and, consequently, in low noise characteristics. A large product of the electron mobility and the electron lifetime (i.e., $\mu_e\tau_e$ between $\sim 5 \times 10^{-3}$ and $10^{-2}\,cm^2/V$, typically) ensures very good electron transport properties resulting in a relatively fast and a high electron collection. However, it has poor charge transport characteristics for holes, which are much slower than electrons, and, worse than that, a large hole trapping probability. Hence, due to the low product of mobility and lifetime for the holes, there are significant charge losses during the drift under a bias electric field. In a simple planar ionization detector, this introduces a dependence of the amplitude of the charge signal collected at the anode on the point of interaction of the gamma-ray in the detector. In the pulse height spectrum, this translates into a broadening of the photopeak, many events showing up in a long low-energy tail (Squillante et al., 2001). In the context of medical gamma-imaging this poses a dilemma. If one reduces the contribution from photons scattered in the body, by using a narrow energy window around the photopeak, one loses efficiency prohibitively. Oppositely, in order to increase the efficiency, a larger energy window has to be used what leads to a deterioration of the image contrast, and makes it impossible to take advantage of the good energy resolution of CdZnTe.

For gamma-ray imaging, segmentation of the readout electrode is required in order to obtain a position resolution as good as possible. The most straightforward method is depicted in Fig. 2. Metal layers are deposited on the two opposite sides of the CdZnTe slab, the layer being continuous on one side but divided into pads on the other. A negative bias voltage is applied to the continuous electrode, while the pixels kept at ground potential are read individually. The fine segmentation of the anode, besides providing position resolution, has an excellent "side-effect" on the pulse height spectrum. As

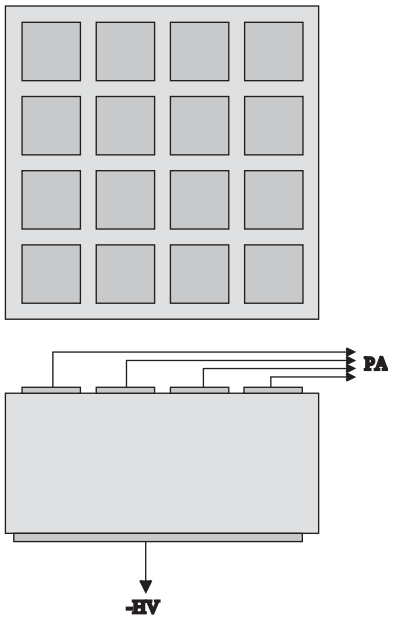

Fig. 2. Schematic drawing of a pixelated block detector of CdZnTe. HV: high voltage; PA: preamplifier, one per pixel.

the induced charge signal in a pixel is mostly due to the motion of the electrons close to it, the dependence of the signal amplitude due to incomplete charge collection of the holes is significantly reduced (Barret et al., 1995). The smaller the ratio of the pixel size to thickness of the detector, the more pronounced is this effect, usually referred to as the "small pixel effect". The drawback of this configuration is that charge is also induced in the pixels adjacent to the collecting one, which increases as the pixel pitch decreases. Hence, several additional correction schemes have been developed and successfully implemented, resulting in excellent energy resolution and a high efficiency in the photopeak (Shor et al., 1999; Verger et al., 2001).

Another approach was followed by Butler (1997) who suggested a different electrode segmentation scheme, which also produces pulse height spectra almost unaffected by the hole trapping.

Several small-field gamma-ray imaging systems based on that type of detectors are being developed for medical applications (Scheiber and Giakos, 2001), some of them by the leading manufacturers of nuclear medicine instrumentation and at least one is already in the market (Butler et al., 1998). They have a modular structure, being composed of pixelated blocks (number of pixels vary between 4×4 and 8×8 per block), each bond directly to the integrated circuit that contains the front-end electronics. The intrinsic spatial resolution is determined by the pixel size which depends on the specific application for which the chamber was designed. Typically, it ranges from a few millimetres (the most common) to a few hundred microns (Kastis et al., 2000). The energy resolution is usually between 4% and 8% for 140 keV gamma-rays, the value depending on the ratio of pixel area to semiconductor slab thickness and on the correction algorithm used (Verger et al., 2001). The detection efficiency is lower than that of the conventional Anger camera: for 140 keV gamma-rays varies typically from 60% to 80%, depending not only on the thickness of the semiconductor slab but also on the correction method (Mestais et al., 2001; Verger et al., 2001).

Their performance characteristics, especially the good position and energy resolution, together with their compactness make them very promising for scintimammography and radiosurgery guidance (Scheiber and Giakos, 2001; Bertolucci et al., 2002). Their mobility and flexibility make them very useful for ambulatory assistance and other situations in which camera has to be transported close to the patient.

Their main drawbacks are the cost and the modest efficiency. The control of inhomogeneities and defects during CdZnTe production is under development.

Besides crystals and semiconductors, other detector technologies have been suggested and pursued. Among them, liquid xenon has been recognized long ago as a very good gamma-ray detector medium. Recently, we reported the successful operation of a liquid xenon ionization chamber with imaging capability (Solovov et al., 2002b). Although liquid xenon is also a very good scintillator, the proposed detector only relies on the charge signal available upon direct conversion of the gamma-rays in the xenon. This concept avoids the disadvantages inherent to any scintillator-based device. The chamber has a bidimensional charge readout, $50\times50\,mm^2$, consisting of a mini-strip plate made of a glass slab with metal strips deposited along two perpendicular directions (Solovov et al., 2002a). First, results already showed the feasibility of the concept and the possibility of obtaining a position resolution better than 2 mm for 122 keV gamma-rays (Solovov et al., 2002b).

3. Positron emission tomography (PET)

PET uses biologically active tracers labeled with a positron-emitting isotope. The principle of the technique is schematically depicted in Fig. 3. Following the decay of the radioisotope, the positron annihilates with a nearby electron emitting two nearly collinear 511 keV γ-rays. The detection of these two photons in coincidence defines a line along which the emission point is known to be located. By accumulating many annihilation events, the spatial distribution of the isotope, and therefore of the labeled radiopharmaceutical, is reconstructed using algorithms similar to those used in

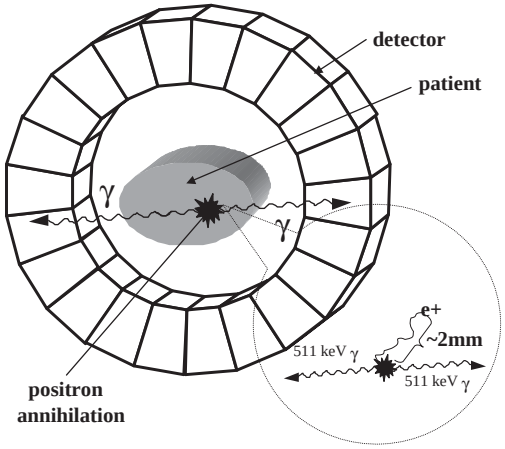

Fig. 3. Schematic diagram of a ring of gamma detectors of a PET scanner. The inset schematically shows that the positron emission location does not coincide with the emission point of the two nearly co-linear 511 keV γ-rays resulting from the annihilation of the thermalized positron with an electron.

transmission tomography and SPECT. Because the detection in coincidence of the two collinear 511 keV γ-rays limits the position of the source to a line, there is no need of a collimator which is one of the great advantages of PET.

In most of the clinical PET scanners, identical γ-ray detector modules are packed as close as possible forming concentric rings whose dimensions depend on the main clinical application of the tomograph. Each individual detector module must exhibit high efficiency for 511 keV γ-ray; spatial resolution of the order of a few millimetres along two directions (corresponding to the axial and transaxial directions of the scanner); good time resolution; low dead time; good energy resolution and low price. The discussion of the importance of these benchmarks can be found, for instance, in Moses et al. (1994).

Presently, the majority of commercial PET systems use, as detector modules, blocks of BGO crystals coupled to four photomultipliers. Each block is partially cut in the direction perpendicular to the PMTs window forming a matrix of pseudo-discrete elements. The scintillation light from each element is shared among the PMTs in a unique way so that the amplitude of their signals can be used to determine the element where the interaction took place (Casey and Nutt, 1986; Tornai et al., 1994). With such BGO detector modules, spatial resolution along the transaxial and axial directions of 5 mm, time resolution of 2 ns, energy resolution of 20% and detection efficiency of 80% have been obtained (Moses, 2001). However, these figures of merit seem to represent the best performance achievable with this technology due to the low light yield of BGO (see Table 3) which limits not only the energy resolution but also the number of crystals that can be unambiguously decoded (and thus their size and consequently the position resolution). Another drawback of BGO is the decay time of the light emission. A faster scintillator would improve the time resolution, reducing the accidental coincidences, and decrease the dead time. However, the strongest limitation of this technology is the absence of depth of interaction information (DOI) of the photons along the crystals. This requirement, which, in principle, is not absolutely necessary for obtaining the image, arises from the need to correct for the degradation of position resolution that occurs gradually from the centre to the edge of the field-of-view of the PET scanner. The off centre γ-rays that enter the crystals at an oblique angle, penetrate into adjacent crystals before interacting (due to the exponential absorption) and therefore can be mispositioned, i.e. assigned to a wrong line, which does not pass through the annihilation point. Presently, this problem is addressed in commercial systems by oversizing the ring diameter so that the central area, where the DOI effect is minimal, is large enough and thus the spatial resolution is fairly uniform. However, the price of the system can be substantially reduced and their performance improved if the PET scanner detectors would provide DOI information. In fact, if the depth of interaction of the γ-ray within the detector module is known, the line passing through the γ-ray emission point in the body will be correctly identified. Thus, the spatial resolution becomes nearly uniform throughout the entire field of view the scanner ring even for very thin and long detector modules.

Recent developments of new PET detector modules and scanner designs have followed three main trends:

(1) Providing general purpose PET systems with DOI information.

(2) Designing detector modules and scanners for specific purposes, namely brain, breast, prostate and small animal imaging. For these applications, detectors with very high space resolution, approaching the limit imposed by the range of the positron before annihilation, are required.

(3) Constructing cameras capable of performing two different types of imaging modalities in the same scanner, such as, for example, PET and X-ray tomography. The advantage of this combination is that PET provides information on the tissue functioning while the X-ray tomography gives a high-resolution image of the object morphology.

Some crystals recently developed have opened up the possibility of both improving the position resolution of PET detectors and implementing some of the DOI determination techniques that have been suggested in last years. As one can see in Table 1, where the commercial acronyms are explained, LSO, GSO, YAP and LuAP are fast scintillators, having a suitable set of properties for being potentially used in PET scanners: LSO is particularly attractive.

Among the numerous schemes for determining the depth at which the interaction took place in crystal-based detector modules, two have been already implemented in research scanners. They are schematically depicted in Fig. 4. One consists in using blocks similar to those of the conventional scanners but made of two or more scintillators with different decay times (they are referred usually as "phoswich" detector blocks). By providing the readout electronics with pulse shape discrimination capability, the type of scintillator where the interaction occurred is identified. This gives a rough information on the depth of the interaction which depends on the thickness of each layer. In the other technique, opposing sides of a block of small optically isolated crystals are coupled to two photodetectors, as for instance a photomultiplier and an array of silicon photodiodes. The depth of the interaction is estimated from the ratio of the two photodetector signals.

Despite the dominant use of crystals in PET scanners and in view of their limitations, other detector technologies are being developed, as for instance various types of gas detectors, which have the drawback of low efficiency but are intrinsically homogeneous, can achieve excellent position resolution and can provide DOI information (or are even free of parallax error), at low price (Parker et al., 2002; Blanco et al., 2003). An additional advantage of the system described in Blanco et al. (2003) is that, owing to an extremely good time resolution, the γ-ray time-of-flight can be used for the reconstruction.

Liquid xenon presents good charge transport and gamma-ray attenuation properties besides being an excellent scintillator and intrinsically homogeneous. Its drawback is that it requires low-temperature operation, around -100°C. We have developed a PET detector based on small liquid xenon cells, as depicted in Fig. 5. They are 10 mm in width (x, the transaxial direction), 50 mm in depth (z, the radial direction) and 60 mm in length (y, the axial direction), separated by stainless-steel planes (0.5 mm thick) that work as cathodes. The anode plane in the middle of each cell was initially formed by 20 wires stretched along the y-direction with a pitch of 2.5 mm and connected into pairs but it will be replaced by a 2D-strip plate similar to that used in the gamma camera described above (Solovov et al., 2002a, b).

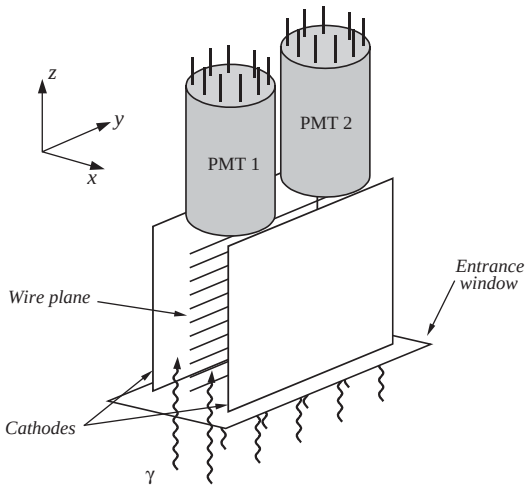

Fig. 5. Schematic representation of a liquid xenon chamber for a PET detector.

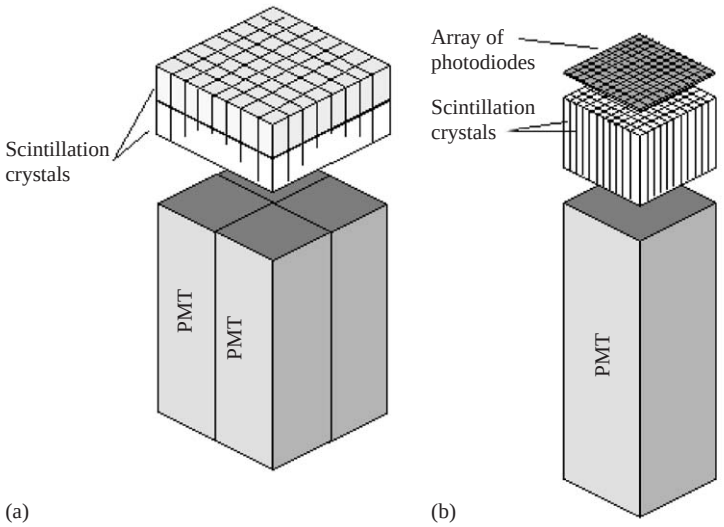

Fig. 4. Two methods of determining the depth of interaction within crystals: (a) using a block made of two layers of crystals with different decay times; (b) by the sharing of the light among a photomultiplier and an array of silicon photodiodes coupled to the opposite sides of a block of optically isolated crystals.

Table 4
Comparison of the liquid xenon detector with two scintillation crystal systems for PET. All resolutions are FWHM

	LXe module	BGO block detector[a]	LSO block detector[b,c]
Time resolution (ns)	1.3	2	1.5
Position resolution[d] (mm)	0.8	5	2
DOI capability[e] (mm)	2–5	None	7.5
Energy resolution (%)	15–17	20	14–20
Efficiency (%)	60	80	Not quoted
Dead time[f] ($\mu s\,cm^2$)	50	25	Not quoted

[a] Moses (2001).
[b] Schmand et al. (1998).
[c] Wienhard et al. (2002).
[d] Along the axial and transaxial directions.
[e] DOI stands for depth of interaction.
[f] Product of the dead time and the detector area that becomes dead by a gamma interaction.

Charge signals induced on the wires are read individually. The depth of interaction is given directly by the position along z of the wire that has the signal. The transaxial coordinate is obtained by measuring the drift time of the ionization electrons. The scintillation light is detected by two photomultipliers that overview three cells (to reduce the number of PMTs required). The fast signal taken from their last dynode is used for coincidence and as the trigger for event processing, namely for starting the electrons drift time measurement. The localization in the y-direction can be measured using the ratio between the amplitudes of the two PMTs, but the resolution, being reasonable in the upper part of the chamber, degrades significantly down to the bottom. This problem can be solved by replacing the wire plane with the mini-strip plate described above, which intrinsically has already position sensitivity in two dimensions, y and z in this case. Table 4 summarizes the results of assessment of the liquid xenon module in comparison with two state-of-the-art scintillation detectors. More details on the detector and its performance are given in Chepel et al. (1999), Crespo et al. (2000) and Lopes et al. (2001).

4. Dual modality

Presently, there is a strong interest in the development of systems capable of providing images of the same object taken with more than one technique, those combining X-ray and radionuclide imaging being particularly appealing. The easiest approach to this problem is to build systems that comprise two aligned scanners, one placed after the other around a single bed, so that two images taken using different modalities can be obtained without repositioning the patient (Beyer et al., 2000). These devices combine techniques that give complementary information. For example, X-ray-computed tomography provides detailed anatomical images with very good position resolution, while PET gives biochemical and functional information. The merging of the images from both scanners allows a much more accurate diagnosis and can provide substantial additional information (Hasegawa et al., 2001). Very recently, systems of this type have started to be commercialized and to be used in nuclear medicine centres and hospitals.

Another approach to the problem is to have a single detector system that can acquire the images of both modalities with the patient exactly in the same position. For instance, this is the case of a dedicated breast imaging system, which is able to provide both an X-ray mammography and a planar scintigram keeping the same compressed position of the breast (Goode et al., 1999).

A further trend in dual modality imaging instrumentation is to use adapted dual-head gamma camera systems not only for scintigraphy and SPECT but also to acquire PET images by removing the collimator and operating in coincidence mode (Patton et al., 2000). There are also systems which are able to provide CT images by adding an X-ray tube (Kimiaei and Larsson, 1996; Patton et al., 2000). Obviously, this flexibility is obtained at the expense of a compromise between the performances of the device for each modality. The main motivation for developing such systems is mostly economic since dedicated PET scanners are quite expensive and some clinical situations do not really require the high-quality images they provide.

5. Conclusions

The recent development of detector crystals, position-sensitive photodetectors and semiconductors has had an enormous impact on the medical radioisotope imaging instrumentation. New compact gamma cameras, with high resolution and optimized for specific applications, such as scinti-mammography, animal imaging and surgical probes, based on CZT or crystals, are already in the market or are being in an advance stage of development. As for PET, the goal of providing the crystal-based scanners with DOI information have found some viable solutions that are being improved and implemented. Among other technologies, a liquid xenon detector module with excellent position resolution and fine DOI information is very promising. The development of new positron emission mammography (PEM) and small animal systems is particularly lively, as is the design and construction of multimodality devices.

Acknowledgements

This work was financed by Project PRAXIS XXI/2./2.1/SAU/1342/95 from Fundação para a Ciência e Tecnologia, Portugal.

References

Anger, H.O., 1958. Scintillation camera. Rev. Sci. Instr. 29, 27–33.

Barret, H.H., Eskin, J.D., Barber, H.B., 1995. Charge transport in arrays of semiconductor gamma-ray detectors. Phys. Rev. Lett. 75 (1), 156–159.

Berger, M.J., Hubbell, J.H., Seltzer, S.M., Coursey, J.S., Zucker, D.S., 1999. XCOM: photon cross section database (version 1.2). Available online: http://physics.nist.gov/xcom.

Bertolucci, E., Maiorino, M., Mettivier, G., Montesi, M.C., Russo, P., 2002. Preliminary test of an imaging probe for nuclear medicine using hybrid pixel detectors. Nucl. Instrum. Methods A 487, 193–201.

Beyer, T., et al., 2000. A combined PET/CT scanner for clinical oncology. J. Nucl. Med. 41, 1369–1379.

Blanco, A., Chepel, V., Marques, R.F., Fonte, P., Lopes, M.I., Peskov, V., Policarpo, A., 2003. Perspectives for positron emission tomography with RPCs. Nucl. Instrum. Methods A 508, 88–93.

Bolozdynya, A., Egorov, V., Koutchenkov, A., et al., 1997. A high pressure xenon self-triggered scintillation drift chamber with 3 D sensitivity in the range 20–140 keV deposited energy. Nucl. Instrum. Methods A 385, 225–238.

Butler, J.F., 1997. Novel electrode design for single-carrier charge collection in semiconductor nuclear radiation detectors. Nucl. Instrum. Methods A 396, 427–430.

Butler, J.F., et al., 1998. CdZnTe solid-state gamma camera. IEEE Trans. Nucl. Sci. 45 (3), 359–363.

Casey, M.E., Nutt, R., 1986. A multicrystal two dimensional BGO detector system for positron emission tomography. IEEE Trans. Nucl. Sci. 37, 460–463.

Chepel, V., Solovov, V., van der Marel, J., Lopes, M.I., Crespo, P., Janeiro, L., et al., 1999. The liquid xenon detector for PET: recent results. IEEE Trans. Nucl. Sci. 46 (4), 1038–1044.

Crespo, P., van der Marel, J., Chepel, V., Lopes, M.I., Janeiro, L., Dinis, S., et al., 2000. Pulse processing for the PET liquid xenon multiwire chamber. IEEE Trans. Nucl. Sci. 47, 2119–2126.

Egorov, V.V., Miroshnichenko, V.P., Rodionov, B.U., Bolozdynya, A.I., Kalashnikov, S.D., Krivoshein, V.L., 1983. Electroluminescence emission gamma-camera. Nucl. Instrum. Methods 205, 373–374.

Goode, A.R., et al., 1999. A system for dual modality breast imaging. In: Anthony Seibert, J. (Ed.), 1999 IEEE Nuclear Science Symposium and Medical Imaging Conference. Seattle.

Hasegawa, B., Tang, H.R., Da Silva, A.J., Wong, K.H., Iwata, Koji., Wu, M.C., 2001. Dual-modality imaging. Nucl. Instrum. Methods A 471, 140–144.

Kastis, G.A., et al., 2000. Gamma-ray imaging using a CdZnTe Pixel array and a high resolution parallel-hole collimator. IEEE Trans. Nucl. Sci. 47 (6), 1923–1927.

Kimiaei, S., Larsson, S.A., 1996. Simultaneous SPECT and CT with an opposed dual head gamma camera system and conventional parallel hole collimators. IEEE Trans. Nucl. Sci. 43 (4), 2239–2243.

Knoll, G.F., 2000. Radiation Detection and Measurement. Wiley, New York.

Lima, J.J.P., 1998. Radioisotopes in medicine. Eur. J. Phys. 19, 485–497.

Lopes, M.I., Chepel, V., Solovov, V., Marques, R.F., Policarpo, A., 2001. Positron emission tomography instrumentation: development of a detector based on liquid xenon. In: Barreira, G., et al. (Ed.), Proceedings of Calor99—VIII International Conference on Calorimetry in High Energy Physics, Lisboa, Portugal. Word Scientific, Singapore, pp. 675–680.

Maini, C.L., et al., 1999. ^{99m}Tc-MIBI scintimammography using a dedicated nuclear mammograph. J. Nucl. Med. 40 (1), 46–51.

Mestais, C., et al., 2001. A new design for a high resolution, high efficiency CZT gamma camera detector. Nucl. Instrum. Methods A 458, 62–67.

Moses, W.W., 2001. Trends in PET imaging. Nucl. Instrum. Methods A 471, 209–214.

Moses, W.W., Derenzo, S.E., Budinger, T.F., 1994. PET detector modules based on novel detector technologies. Nucl. Instrum. Methods A 353, 189–194.

Nguen Ngoc, H., Jeanjean, J., Itoh, H., Charpak, G., 1980. A xenon high-pressure proportional scintillation camera for X and γ-ray imaging. Nucl. Instrum. Methods 172, 603–608.

Notaristefani, F., et al., 1996. First results from YAP:Ce gamma camera for small animal studies. Trans. Nucl. Sci. 43 (6), 3264–3270.

Pani, R., et al., 1998. Dedicated gamma camera for single photon emission mammography (SPEM). Trans. Nucl. Sci. 45 (6), 3127–3133.

Parker, D.J., Forster, R.N., Fowles, P., Takhar, P.S., 2002. Positron emission particle tracking using Birmingham positron camera. Nucl. Instrum. Methods A 477, 540–545.

Patton, J.A., Delbeke, D., Sandler, M.P., 2000. Image fusion using an integrated dual-head coincidence camera with X-ray tube based attenuation maps. J. Nucl. Med. 41, 1364–1379.

Scheiber, C., Giakos, G., 2001. Medical applications of CdTe and CdZnTe detectors. Nucl. Instrum. Methods A 458, 12–25.

Schmand, M., Erikson, L., Cassey, M.E., Andreaco, M.S., Melcher, C., Wienhard, K., Flugge, G., Nutt, R., 1998. Performance results of a new DOI detector block for a high resolution PET—LSO research tomograph HRRT. IEEE Trans. Nucl. Sci. NS-45, 3000–3006.

Shor, A., Eisen, Y., Mardor, I., 1999. Optimum spectroscopic performance from CZT γ- and X-ray detectors with pad and strip segmentation. Nucl. Instrum. Methods A 428, 182–192.

Solovov, V., Chepel, V., Pereira, A., Lopes, M.I., Marques, R.F., Policarpo, A.J.P.L., 2002a. Two dimensional readout in a liquid xenon ionization chamber. Nucl. Instrum. Methods A 477, 184–190.

Solovov, V., Chepel, V., Lopes, M.I., Neves, F., Marques, R.F., Policarpo, A.J.P.L., 2002b. Liquid xenon γ-camera with ionization readout. Nucl. Instrum. Methods A 478, 435–439.

Squillante, M.R., Cirignano, L., Grazioso, R., 2001. Room temperature semiconductor device and array configurations. Nucl. Instrum. Methods A 458, 288–296.

Tornai, M.P., Germano, T.M., Hoffmman, E.J., 1994. Positioning and energy response of PET block detectors with different light sharing schemes. IEEE Trans. Nucl. Sci. 41 (4), 1458.

Van Eijk, C., 2001. Inorganic-scintillator development. Nucl. Instrum. Methods A 460, 1–14.

Verger, L., et al., 2001. Characterization of CdTe and CdZnTe detectors for gamma-ray imaging applications. Nucl. Instrum. Methods A 458, 297–309.

Webb, S., 1998. The Physics of Medical Imaging. IOP Publishing, London.

Wienhard, K., et al., 2002. The ECAT HRRT: performance and first clinical application of the new high resolution research tomograph. IEEE Trans. Nucl. Sci. 49 (1), 104–110.